AGU PUBLICATIONS

Geophysical Research Letters

RESEARCH LETTER
10.1002/2014GL061773

Key Points:
- New global Mean Dynamic Topography from GOCE, altimetry, and in situ data
- New two-level Ekman model from the joint analysis of Argo floats and SVP drifters
- New ocean currents by combining geostrophy and Ekman at surface and 15 m depth

Correspondence to:
M.-H. Rio,
mrio@cls.fr

Citation:
Rio, M.-H., S. Mulet, and N. Picot (2014), Beyond GOCE for the ocean circulation estimate: Synergetic use of altimetry, gravimetry, and in situ data provides new insight into geostrophic and Ekman currents, *Geophys. Res. Lett.*, *41*, 8918–8925, doi:10.1002/2014GL061773.

Received 5 SEP 2014
Accepted 18 NOV 2014
Accepted article online 21 NOV 2014
Published online 18 DEC 2014

Beyond GOCE for the ocean circulation estimate: Synergetic use of altimetry, gravimetry, and in situ data provides new insight into geostrophic and Ekman currents

M.-H. Rio[1], S. Mulet[1], and N. Picot[2]

[1]CLS, Ramonville Saint-Agne, France, [2]CNES, Toulouse, France

Abstract Accurate estimate of ocean surface currents is both a challenging issue and a growing end-users requirement. In this paper ocean currents are calculated at two levels (surface and 15 m depth) as the sum of the geostrophic and Ekman components. First, a new, global, $\frac{1}{4}^{\circ}$ Mean Dynamic Topography, called the CNES-CLS13 MDT, has been calculated and is now available for use by the oceanographic community. By exploiting information from surface drifters and Argo floats, the new MDT resolves spatial scales beyond the resolution permitted by the recent Gravity and Ocean Circulation Experiment (GOCE) geoid models (125 km). Associated mean geostrophic speeds in strong currents are increased by 200% on average compared to GOCE-based mean currents. In addition, for the first time, a two-level, monthly, empirical Ekman model that samples a spiral-like behavior is estimated. We show that combining both pieces of information leads to improved ocean currents compared to other existing observed products.

1. Introduction

The estimation of accurate ocean surface currents is crucial for a wide and growing range of applications (offshore industry, search and rescue, oil spill monitoring…). The objective of this paper is to provide a new estimate of ocean surface currents as the sum of two contributions, geostrophic currents and wind-induced Ekman currents. This first-order approximation is also the approach used to calculate the OSCAR (Ocean Surface Current Analysis Real Time) [*Bonjean and Lagerloef*, 2002; *Dohan and Maximenko*, 2010] or the GEKCO (Geostrophic and Ekman Current Observatory) [*Sudre and Morrow*, 2008; *Sudre et al*., 2013] products. In both products, the geostrophic component is obtained by deriving altimeter maps of the ocean absolute dynamic topography, calculated as the sum of the altimeter Sea Level Anomalies (SLA) and an ocean Mean Dynamic Topography (MDT). A number of studies have demonstrated the importance of the recent GOCE (Gravity and Ocean Circulation Experiment) mission for calculating the ocean MDT [*Bingham et al*., 2011; *Knudsen et al*., 2011; *Mulet et al*., 2012; *Becker et al*., 2014]. The resulting fields are accurate at the centimeter level at scales of around 100–150 km [*Mulet et al*., 2012], which is a significant improvement over the previous Gravity Recovery and Climate Experiment (GRACE)-based geoid models. However, considering the values of the first deformation Rossby radius [*Chelton et al*., 1998], we expect the MDT to contain shorter scales and external information is needed in order to resolve them.

Small-scale structures can be recovered by using in situ measurements [*Rio and Hernandez*, 2003; *Maximenko et al*., 2009]. This approach was applied by *Rio et al*. [2011] to compute the CNES-CLS09 MDT, used in particular to calculate the geostrophic component of the OSCAR and GEKCO products. However, this solution is based on a geoid model calculated from GRACE data and on a data set of drifting buoy velocities distributed by the Surface Drifter Data Assembly Center (SD-DAC) that has been demonstrated subsequently to be highly polluted by undetected undrogued drifters [*Grodsky et al*., 2011]. Those data are significantly impacted by direct wind slippage in addition to the advection by ocean surface currents [*Rio*, 2012]. There is therefore an urgent need to provide the altimeter data user community with an updated solution that benefits both from the newly highly accurate GOCE data and from an entire reprocessing of the drifter data set. This newly computed CNES-CLS13 MDT is presented in section 2.

In the open ocean, the second major contribution to the ocean surface currents after geostrophy is the Ekman response of the ocean to wind stress. A number of studies have focused on the better understanding

and modeling of these currents [*Ralph and Niiler*, 1999; *Lagerloef et al*., 1999; *Elipot and Gille*, 2009; *Rio et al*., 2003, 2011, 2012]. *Liu et al*. [2014] have shown the positive impact of taking this component into account for Lagrangian studies. In OSCAR, Ekman currents are estimated using an Ekman/Stommel formulation with variable eddy viscosity using National Centers for Environmental Prediction winds. In GEKCO, an empirical, latitudinal dependent Ekman model is used whose two parameters, the Ekman layer depth and the vertical viscosity, are estimated by linear fit between Ekman velocities extracted from drifter velocities and winds from the NASA Quick Scatterometer (QuickSCAT) mission [*Sudre et al*., 2013].

In this paper, for the first time, an empirical Ekman model is calculated for two specific depths (surface and 15 m) with a parameter dependency on latitude, longitude, and month (section 2). This model is needed, first, for the processing of the drifter velocities used in the CNES-CLS13 MDT computation, and second, for the calculation of the Ekman current maps, that, added to the maps of geostrophic currents, result in a new 1993–2012 data set of 3-hourly, global ocean currents at the surface and at 15 m depth. This new data set is presented in section 3 and compared to other existing ocean current products.

2. Data and Method

2.1. Data

This paper is based on the synergy of altimetry, gravimetry, and in situ data. The Ssalto/Duacs delayed-time multimission maps of altimeter height and geostrophic velocity anomalies distributed by Archiving, Validation, and Interpretation of Satellite Oceanographic data (AVISO) for the period 1993–2012 have been used, as well as the CNES-CLS11 altimeter Mean Sea Surface (MSS) from *Schaeffer et al*. [2012]. This MSS was selected because of its consistency with the altimeter SLA regarding both altimeter data processing and the time reference period (1993–1999). For the geoid, we used the latest version of the GOCE model available at the time of the study, the EGM-DIR R4 model [*Bruinsma et al*., 2013]. The in situ data sets consist of hydrological profiles measured by Argo floats and conductivity-temperature-depth casts from the Coriolis Ocean database ReAnalysis (CORA3.4) covering the years 1993 to 2012 [*Cabanes et al*., 2013], Surface Velocity Program (SVP) drifting buoy data distributed in delayed time by the SD-DAC from January 1993 to September 2012, and for which the drogue loss date has been recently reevaluated [*Lumpkin et al*., 2012], and Argo float surface velocities from the YoMaHa'07 (Yoshinari Maximenko Hacker) data set [*Lebedev et al*., 2007] covering the 2000–2013 period. Also, the 3-hourly wind stress data from the ERA-Interim reanalysis [*Simmons et al*., 2007] have been used.

2.2. CNES-CLS13 MDT Calculation

The method used to compute the CNES-CLS13 MDT has been described in detail in previous papers [*Rio et al*., 2011]. The first step is to compute a so-called "geodetic MDT" by subtracting the geoid model from the altimeter MSS. The raw difference between the two surfaces is polluted by both commission and omission errors on the geoid model, and further filtering is required. Isotropic Gaussian filters fail to separate the different error contributions. Instead, as in *Rio et al*. [2011], an optimal filter is applied. This approach is based on the objective analysis method [*Bretherton et al*., 1976] in which the output field is a weighted mean of the observations (here the raw MSS minus geoid heights). The weights depend on the observation errors and the a priori variance and correlation scales of the signal. The resulting smoothed geodetic MDT is shown in Figure 1a.

To improve the geodetic MDT resolution, estimates of the mean heights and mean geostrophic velocities are built from in situ measurements of the ocean dynamic heights and current velocities from which the temporal variability measured by altimetry is removed [*Rio et al*., 2011]. In situ data are processed to make them consistent with the physical signal measured by altimetry: absolute dynamic heights are reconstructed from the in situ steric dynamic heights, and the geostrophic component of the ocean currents is extracted from the drifter velocities. In the case of the dynamic heights, the exact same processing as in *Rio et al*. [2011] was applied. For the surface velocities, however, a new approach has been explored that takes into account the information from both the drogued and undrogued drifters (thereby more than doubling the number of available velocity measurements compared to the use of drogued drifters only as was done in *Rio et al*. [2011]). SVP drifters are composed of a surface float connected to a subsurface 7 m long holey-sock drogue centered at 15 m depth. This design was conceived to minimize the wind slippage so that the drogued drifters follow the currents at 15 m depth [*Niiler et al*., 1987, 1995]. In case of drogue loss, the drifter is advected by the surface currents and in addition, is subject to wind

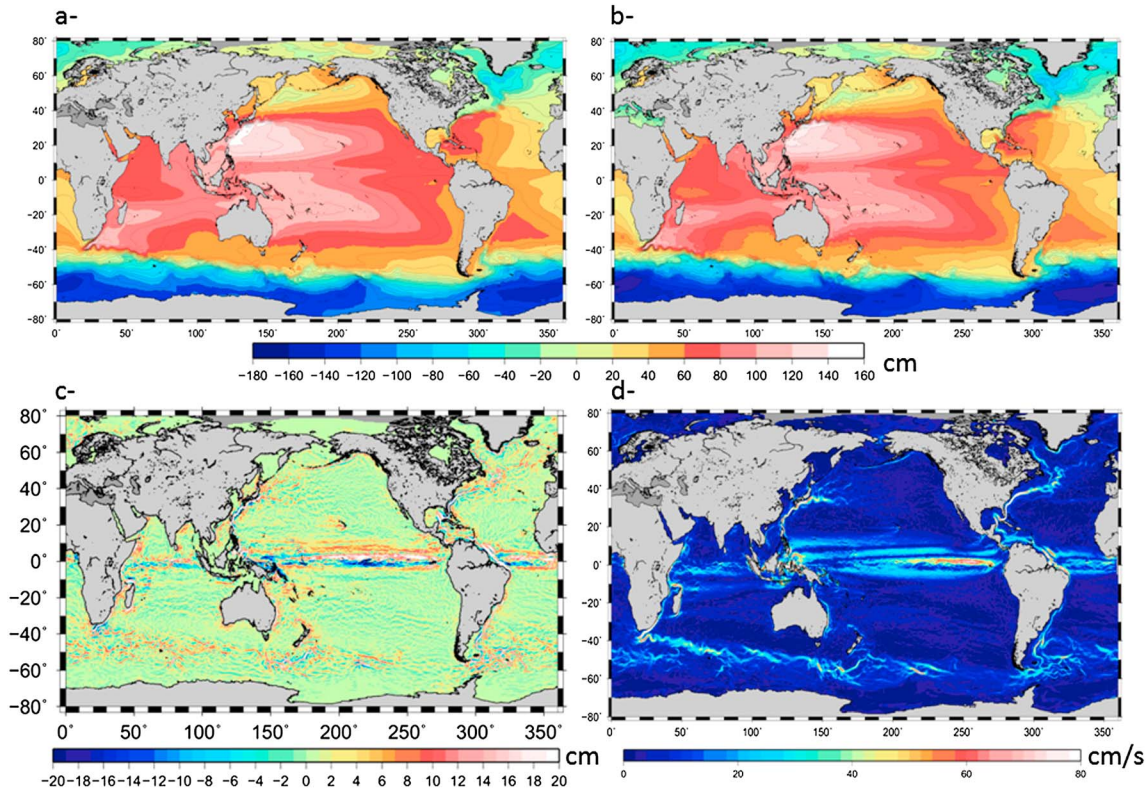

Figure 1. (a) The GOCE-based geodetic MDT used as first guess. (b) The CNES-CLS13 MDT (cm). (c) Differences (cm/s) between the mean geostrophic velocity speed from the CNES-CLS13 MDT and from the GOCE-based first guess. (d) The mean circulation (cm/s) from the CNES-CLS13 MDT.

slippage. The extraction of the geostrophic velocity component from the SVP drifter velocities thus implies removing Ekman currents at 15 m depth for drogued drifters and removing Ekman currents at the surface plus the wind slippage for undrogued drifters.

Consequently, a new, two-level (surface and 15 m) Ekman model was estimated (section 2.3) and used to calculate Ekman currents along the drifter trajectories. The surface Ekman component was then subtracted from the undrogued drifter velocities and the 15 m depth Ekman component from the drogued drifter velocity. Also, the drifter velocities were corrected from wind slippage using the method from *Rio* [2012]. We find a mean wind slippage lower than 1–2 cm/s everywhere in the case of drogued drifters, while the zonal mean wind slippage calculated for the undrogued drifters locally exceeds 10 cm/s in the Antarctic Circumpolar Current (ACC). Our approach is quite efficient to correct the undrogued drifter velocities from the unwanted Ekman surface current plus wind slippage: the zonal root-mean-square (RMS) difference between altimeter geostrophic velocities (derived from the maps of absolute dynamic heights calculated as the sum of the geodetic MDT and the altimeter SLA) and the drogued SVP drifter velocities is 14.4 cm/s, while the difference with the undrogued drifter velocities is 19.2 cm/s. When correcting the drogued drifters from the 15 m depth Ekman currents, the RMS drops to 13.5 cm/s. When correcting the undrogued drifter velocities from the surface Ekman current only, the zonal RMS difference is still high (14.7 cm/s) and the mean zonal differences are strongly correlated to the mean wind patterns (large positive anomalies in the ACC and negative anomalies in the trade winds area—not shown). Removing also the wind slippage from the undrogued drifter velocities further reduces the zonal RMS difference to 13.5 cm/s. Once the Ekman currents and the wind slippage were removed from the drifter velocities, a 3 day low-pass filter was applied along the drifter trajectories to get rid of the other ageostrophic currents (inertial oscillations, stokes drift, tides…). The chosen cutoff period may be insufficient to fully remove the inertial oscillations for latitudes equatorward of 10°. The geostrophic altimeter velocity anomalies were also interpolated along the buoy trajectories and subtracted from the instantaneous geostrophic velocities to end up with estimates of the mean geostrophic velocities that were finally averaged into 0.25° by 0.25° boxes. An error, calculated as the box

variance divided by the number of observations, was associated with each box mean. This error accounts in particular for the unremoved inertial signal in the (−10°;10°) latitudinal band.

The resulting mean velocities and heights were then used to improve the geodetic MDT through a remove-restore technique: the first guess estimate (geodetic MDT and associated mean geostrophic velocities) is first removed from the mean observations and an objective analysis is performed on the residual heights and velocities [*Rio et al*., 2011]. Then, the first guess is added back to the estimated field. The variance and covariance information needed to map the residuals were computed using the modeled MDT from the GLobal Ocean ReanalYsis and Simulation (GLORYS) reanalysis [*Ferry et al*., 2012]. The zonal/meridian radii decrease from 250/180 km at the equator to 100/100 km at high latitudes. Compared to previous studies by *Rio et al*. [2011], the use of undrogued drifter velocities is both an asset and a challenge. To check for the reliability of using this new data set, we calculated two different MDT solutions using the processed drogued and undrogued mean velocities separately. The global difference between the two resulting MDTs is only about 1 cm RMS.

Quantitative comparison between the two solutions was then performed using the independent YoMaHa surface velocities. These velocities are deduced from the trajectories of the Argo floats during the time spent at the ocean surface to transmit their data (usually between 12 and 24 h). Mean geostrophic velocities were computed from the Argo float surface velocities by removing the Ekman surface currents (section 2.3) and the altimeter geostrophic velocity anomaly. For both solutions (based on drogued or undrogued drifter data), the RMS differences calculated between the derived mean velocities and the Argo float mean velocities are very close (around 14.50 cm/s for the zonal component, which corresponds to 45% of the Argo float velocity variance, and around 14.55 cm/s for the meridional component, which corresponds to 53% of the Argo float velocity variance). This result confirms the validity of using the processed undrogued drifter data set for the CNES-CLS13 MDT computation. We also check that the joint use of the two data sets to compute the MDT leads to increased agreement with the independent Argo mean velocities (values of 44.6% and 52.4% of the Argo float velocity variance were obtained for the zonal and meridional component, respectively).

Finally, we merged all available velocity estimates to produce a single data set of mean velocities from SVP drogued and undrogued drifters and Argo floats. This final data set was used with the mean heights to compute the CNES-CLS13 MDT on a $\frac{1}{4}$° grid. The resulting solution and the associated mean geostrophic velocities are shown in Figures 1b and 1d, respectively. The difference with the first guess (Figure 1c) shows the impact of adding the short scales derived from the in situ observations compared to using only geodetic data. This reveals the very good performance of the GOCE data outside the strong gradient areas: very little additional information is brought by in situ data. On the other hand, it is quite evident that the use of in situ data provides the missing short-scale information in all major western boundary currents and in the equatorial currents. The speed of those currents is doubled on average, and the associated jets are much thinner (see the blue patterns around the red core in Figure 1c for all strong currents). The impact of using this new field instead of other solutions for the calculation of altimeter geostrophic currents will be further highlighted in section 3.

2.3. New Empirical Ekman Model

The modeling of the Ekman currents is based on the approach described in *Rio et al*. [2003; 2011; 2012], generalized to consider different depths *z*.

At depth *z*, the Ekman response of the ocean $\vec{u}_{ek}(z)$ to the wind stress forcing $\vec{\tau}$ is written using a two-parameter ($\beta(z)$, $\theta(z)$) formulation:

$$\vec{u}_{ek}(z) = \beta(z)\,\vec{\tau}\,e^{i\theta(z)} \tag{1}$$

We estimate $\beta(z)$ and $\theta(z)$ at $z = 0$ m and $z = 15$ m by applying a least squares fit between estimates of $\vec{u}_{ek}(z)$ and simultaneous values of the ERA-Interim wind stress $\vec{\tau}$.

To estimate $\vec{u}_{ek}$ ($z = 15$ m), geostrophic velocities were subtracted from the 15 m drogued SVP buoy velocities. The geostrophic velocities were derived from altimeter maps of absolute dynamic topographies obtained adding the large-scale geodetic MDT (section 2) and the SLA maps. In the equatorial band, a Beta-plane approximation is used [*Lagerloef et al*., 1999]. The residual ageostrophic current was further filtered using a P_i (inertial period) to 20 days band-pass filter to focus on the frequencies where the coherency between the

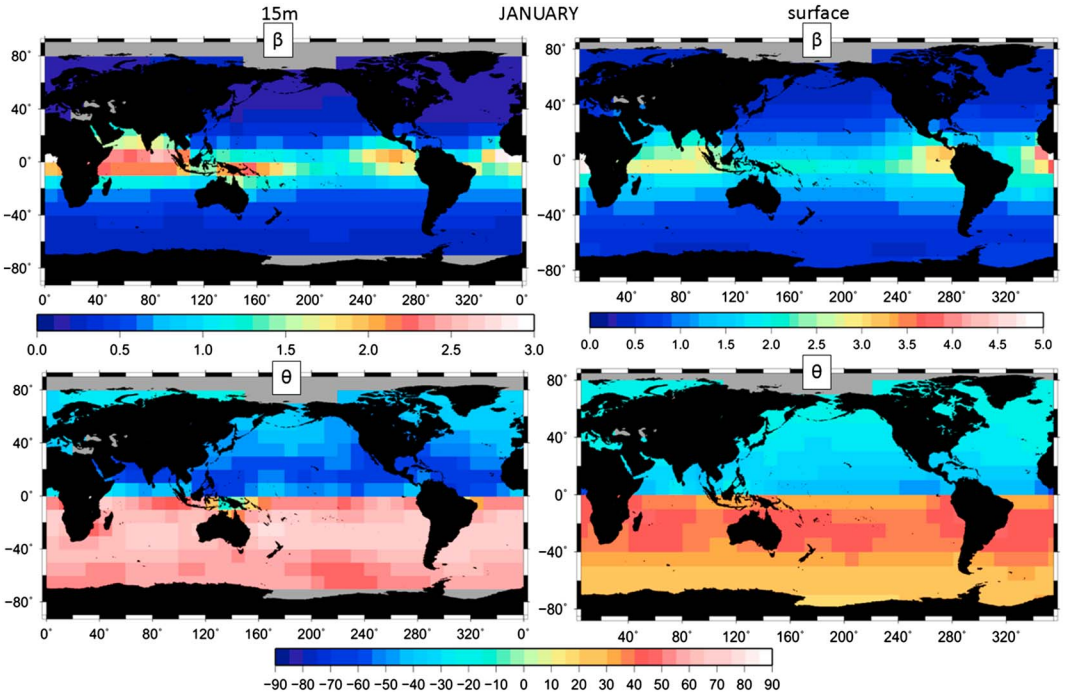

Figure 2. The β (in m^2s/kg) and θ (in °C) parameters of the Ekman model calculated in this study for the month of January from the (left) SVP drogued drifters and from the (right) Argo floats derived velocities.

wind stress and the Ekman currents is maximal [*Rio and Hernandez*, 2003]. At latitudes polarward 5°, P_i is taken as the maximum between 25 h and the inertial oscillations period. At latitudes equatorward of 5°, P_i is equal to $P_i(5°)$.

To estimate $\vec{u}_{ek}$ ($z = 0$ m), the geostrophic velocities were subtracted from the Argo surface velocities. We expect Argo floats to be much less affected by direct wind slippage than the undrogued SVP drifters (this will be confirmed later) and to be reliable tracers of the surface currents. This may be explained by the respective design of both floats: An Argo float is more than 1 m long with a stability disk aiming at stabilizing the float when at the surface to allow for the data transmission to the satellite. A SVP drifter, once the drogue has been lost, is made of a 30 cm diameter surface spherical float that may be much more affected by the wind than an Argo float.

The β and θ parameters were first fitted for the global data sets. At the surface (using the 841,786 Argo floats velocities) the Ekman currents are found to respond to wind stress with an angle of $\theta(z = 0\text{ m}) = 30.75°$ (to the right of the wind direction in the Northern Hemisphere, to the left in the Southern Hemisphere) and an amplitude factor $\beta(z = 0\text{ m}) = 0.61\ m^2s/kg$.

At 15 m depth, using the 7,537,441 SVP drifter velocities, a higher angle was found, in good agreement with an Ekman spiral-like structure of the current shear, $\theta(z = -15\text{ m}) = 48.18°$, and a smaller amplitude factor than at the surface $\beta(z = 15\text{ m}) = 0.25\ m^2s/kg$.

The fit done using the undrogued SVP drifter velocities (10,860,007 velocity measurements) yields an angle response $\theta = 18.25°$ and an amplitude factor $\beta = 0.73\ m^2s/kg$.

These results clearly highlight the different behavior of the Argo floats compared to the undrogued SVP drifters, although both type of drifters are located at the surface of the ocean. The undrogued drifter response is characterized by a higher-amplitude parameter β and a smaller-angle parameter, which confirms that Argo floats are much less affected by wind slippage than undrogued SVP drifters.

From Ekman theory, we expect both parameters to present regional and seasonal variabilities, in correlation with the varying ocean stratification. In order to take into account these variations, we have fitted the two parameters by month and into 4° by 4° boxes. Obtained parameters for the month of January are shown in Figure 2, and the monthly parameters fitted for the global ocean are displayed in Figure 3. The Ekman

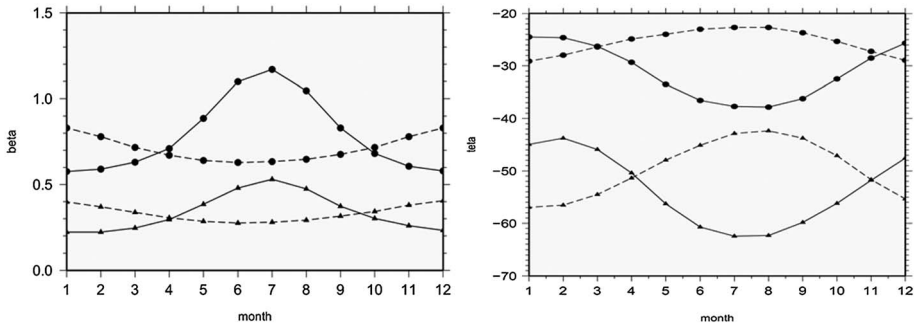

Figure 3. The (left) β (in m^2s/kg) and (right) θ (in °C) parameters fitted for the Northern (solid line) and Southern (dashed line) Hemispheres at the surface (circles) and at 15 m depth (triangles) by month.

response at the surface is located at around 20–40° to the right of the wind direction in the Northern Hemisphere (to the left in the Southern Hemisphere), and the angle then increases to 40–60° at 15 m depth. In addition, a clear seasonal cycle is obtained for both parameters and at both depths with larger angles and amplitudes in summer than in winter (Figure 3), in good consistency with stronger summer stratification. Despite only two levels being sampled, this is the first time an "Ekman spiral-like" response of the ocean currents has been shown at a global scale from in situ observations. Computed angles are smaller than predicted by the Ekman theory (45° at the surface), in which a depth-independent eddy viscosity is considered. Wind-driven, spiraling currents may penetrate well below the mixed layer [*Chereskin*, 1995]. In that case viscosity will change rapidly at the bottom of the mixed layer. Considering a depth dependent eddy viscosity would lead to a smaller angle between the wind direction and the surface current [*Rossby and Montgomery*, 1935]. In addition, because Argo floats remain at the surface only few hours before diving again at depth for around 10 days, we were not able to filter the surface currents from the residual ageostrophic components (inertial oscillations, stokes drift…). *Lewis and Belcher* [2004] showed that introducing a Stokes drift term into the steady state Ekman current equations led to surface current deflections from the wind stress of 10° to 45°, in agreement with our results. Also, *Park et al*., 2005 have shown that the contribution of the inertial currents to the Argo surface velocity may be important. The retrieval of both inertial oscillations and Stokes drift from the Argo floats surface velocities may be an improvement of this work in the future.

3. Result: New Ocean Currents Product

The new CNES-CLS13 MDT and the new two-level Ekman model presented in section 2 were then used, together with the SLA and wind stress data, to calculate, for the period 1993–2012, a data set of daily, $\frac{1}{4}$° maps of geostrophic currents, 0 m and 15 m Ekman currents, and by simple addition, 0 m and 15 m ocean total currents. As an example, Figure 4 shows the resulting currents on 11 February 2012 for an area that includes the strong Agulhas Current and the Benguela Current upwelling system along the western coast of Africa. This plot highlights the strong impact of using the CNES-CLS13 MDT (Figure 4e) instead of the GOCE-based geodetic MDT (Figure 4d) to resolve the Agulhas Current (with maximum velocities exceeding 1.5 m/s, instead of 1 m/s with the GOCE-based geodetic MDT) as well as the importance of resolving also Ekman currents to correctly describe the surface circulation in the Benguela Current area. In this area, the wind often blows northward along the coast (Figure 4a), leading to eastward surface Ekman currents, that push the surface waters away from the coast (Figure 4c), resulting in the upwelling of the underlying colder (Figure 4b, from the Reynolds sea surface temperature products), nutrient-rich waters, that enable high rates of phytoplankton growth and sustain the productive Benguela ecosystem. As shown in Figure 4h, this westward current off Benguela is not resolved in the OSCAR product. This product is an average of the current over the top 30 m, while the 15 m depth Ekman current on that day is significantly reduced compared to its surface intensity (Figures 4c and 4d). Also, the OSCAR Agulhas Current intensity is slightly lower than the intensity resolved using the CNES-CLS13 MDT.

We then performed a quantitative validation of the resulting 15 m depth currents by using an independent data set of 1,804,977 measurements of the ocean currents at 15 m provided by SVP-type drogued drifters processed in near-real time and distributed by the Coriolis data center for the period ranging from September 2012 to September 2013. The global ocean is rather well sampled so that our results are representative of all regions. The drifting buoy velocities have been compared to the collocated 15 m depth

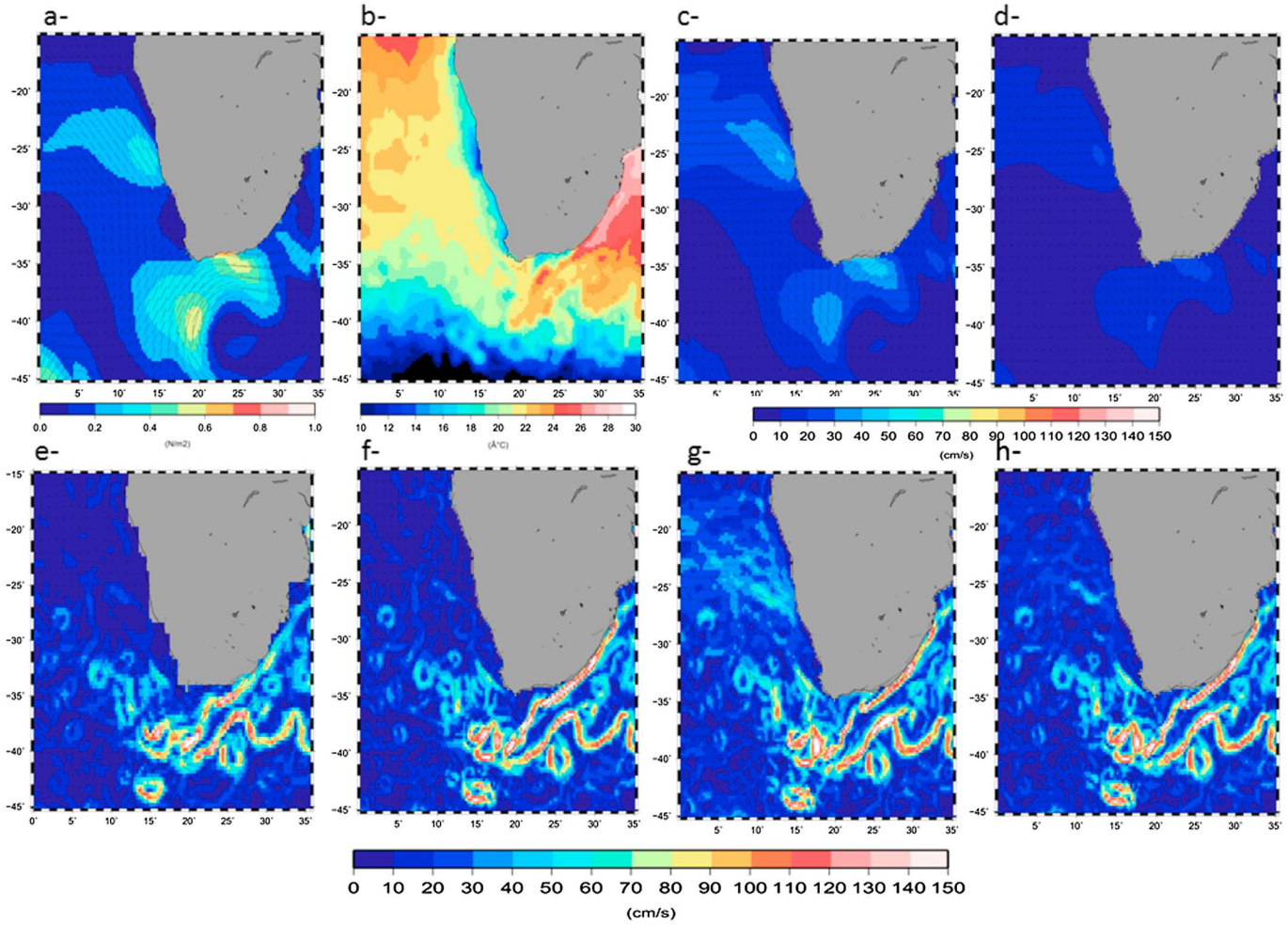

Figure 4. (a) Wind stress (N/m^2) on 11 February 2012. (b) Sea surface temperature (°C). (c) Ekman currents at the surface from the empirical model calculated in this study. (d) Ekman currents at 15 m depth from the empirical model calculated in this study. (e) Geostrophic currents calculated from the sum of altimeter velocity anomalies from AVISO and the GOCE-based geodetic MDT. (f) Geostrophic currents calculated from the sum of altimeter velocity anomalies from AVISO and the CNES-CLS13 MDT. (g) Total currents at the surface calculated as the sum of the surface Ekman currents (Figure 4c) and the geostrophic currents (Figure 4f). (h) OSCAR currents.

velocities. Other currents have been tested, as the OSCAR currents, and also the currents obtained using a different MDT to calculate the geostrophic velocity component (the large-scale geodetic MDT used as first guess, the previous CNES-CLS09 solution, the MDT from *Maximenko et al*. (2009) based on GRACE and drifters, as well as the MDT from the GLORYS2V1 model reanalysis [*Ferry et al*., 2012]). When using the newly computed CNES-CLS13 MDT and the 15 m depth Ekman model, the variance of the zonal differences is reduced to 47.1% of the drifter velocity variance compared to 49% for the CNES-CLS09 MDT, 59.7% for the GOCE-based geodetic MDT, 48.4% for the *Maximenko et al*. [2009] MDT, 49.6% for the GLORYS2V1 MDT, and 54.8% for the OSCAR product. Similarly, the variance of the meridional differences is reduced to 57.8% of the drifter velocity variance compared to 58.5% for the CNES-CLS09 MDT, 64% for the GOCE MDT, 59.3% for the Maximenko MDT, 61.7% for the GLORYS2V1 MDT, and 65% for the OSCAR product.

4. Conclusion

The first major outcome of the work described in this paper is the calculation of a new $\frac{1}{4}^{\circ}$ global Mean Dynamic Topography called the CNES-CLS13 MDT that goes beyond the spatial resolution limitation of the state-of-the-art geoid models based on GRACE and GOCE data, by exploiting the strong synergy between space measurements of gravity and sea level, and in situ measurements of the ocean state. In the future, this merging approach could be extended on a more regional scale to exploit other high-resolution observing systems of the ocean surface currents as the radar HF network or the synthetic aperture radar Doppler velocities.

The second major outcome of this study is the estimation, thanks to the joint use of SVP drifters and Argo floats, of a two-level (surface and 15 m depth) empirical Ekman model that correctly samples, for the first time at global scale, an Ekman-like spiral structure in the ocean.

These two components are combined to provide a new data set of ocean currents at the surface and at 15 m depth, providing an enhanced view of the ocean currents at the near surface compared to other existing products.

Acknowledgments
This study was performed in the framework of a CNES contract and benefited also from the support of the GlobCurrent project from ESA. All data used in this study are freely available and downloadable from the following websites: Altimeter data, http://www.aviso.altimetry.fr/en/data.html; GOCE geoid model, http://icgem.gfz-potsdam.de/ICGEM/modelstab.html; OSCAR currents, http://www.oscar.noaa.gov/datadisplay/oscar_datadownload.php; YoMaHa'07 data set, http://apdrc.soest.hawaii.edu/projects/yomaha/; SVP drifter data set, http://www.aoml.noaa.gov/envids/gld/FtpInterpolatedInstructions.php; and CORA database, http://www.myocean.eu/.

The Editor thanks two anonymous reviewers for their assistance in evaluating this paper.

References

Becker, S., J. M. Brockmann, and W.-D. Schuh (2014), Mean dynamic topography estimates purely based on GOCE gravity field models and altimetry, *Geophys. Res. Lett.*, *41*, 2063–2069, doi:10.1002/2014GL059510.

Bingham, R. J., P. Knudsen, O. Andersen, and R. Pail (2011), An initial estimate of the North Atlantic steady-state geostrophic circulation from GOCE, *Geophys. Res. Lett.*, *38*, L01606, doi:10.1029/2010GL045633.

Bonjean, F., and G. S. E. Lagerloef (2002), Diagnostic model and analysis of the surface currents in the tropical Pacific Ocean, *J. Phys. Oceanogr.*, *32*(10), 2938–2954.

Bretherton, F. P., R. E. Davis, and C. Fandry (1976), A technique for objective analysis and design of oceanographic experiments applied to MODE-73, *Deep-Sea Res. Oceanogr. Abstr.*, *23*(7), 559–582.

Bruinsma, S. L., C. Foerste, O. Abrikosov, J. C. Marty, M.-H. Rio, S. Mulet, and S. Bonvalot (2013), The new ESA satellite-only gravity field model via the direct approach, *Geophys. Res. Lett.*, *40*, 3607–3612, doi:10.1002/grl.50716.

Cabanes, C., et al. (2013), The cora dataset: Validation and diagnostics of in-situ ocean temperature and salinity measurements, *Ocean Sci.*, *9*, 1–18, doi:10.5194/os-9-1-2013.

Chelton, D. B., R. A. de Szoeke, M. G. Schlax, K. El Naggar, and N. Siwertz (1998), Geographical variability of the first baroclinic Rossby radius of deformation, *J. Phys. Oceanogr.*, *28*, 433–459.

Chereskin, T. K. (1995), Evidence for an Ekman balance in the California Current, *J. Geophys. Res.*, *100*, 12,727–12,748.

Dohan, K., and N. Maximenko (2010), Monitoring ocean currents with satellite sensors, *Oceanography*, *23*(4), 94–103, doi:10.5670/oceanog.2010.08.

Elipot, S., and S. T. Gille (2009), Ekman layers in the Southern Ocean: Spectral models and observations, vertical viscosity and boundary-layer depth, *Ocean Sci.*, *5*, 115–139. [Available at http://www.ocean-sci.net/5/115/2009/os-5-115-2009.html.]

Ferry, N., et al. (2012), Reanalysis of the Altimetric Era (1993–2009) at mesoscale, *Mercator Ocean Q. Newsl.*, *44*, 28–39.

Grodsky, S. A., R. Lumpkin, and J. A. Carton (2011), Spurious trends in global surface drifter currents, *Geophys. Res. Lett.*, *38*, L10606, doi:10.1029/2011GL047393.

Knudsen, P., R. Bingham, O. Andersen, and M.-H. Rio (2011), A global mean dynamic topography and ocean circulation estimation using a preliminary GOCE gravity model, *J. Geod.*, *85*, 861–879, doi:10.1007/s00190-011-0485-8.

Lagerloef, G. S. E., G. T. Mitchum, R. B. Lukas, and P. P. Niiler (1999), Tropical Pacific near surface currents estimated from altimeter, wind, and drifter data, *J. Geophys. Res.*, *104*(C10), 23,313–23,326, doi:10.1029/1999JC900197.

Lebedev, K. V., H. Yoshinari, N. A. Maximenko, and P. W. Hacker (2007), YoMaHa'07: Velocity data assessed from trajectories of Argo floats at parking level and at the sea surface IPRC Tech. Note 4, 12 June.

Lewis, D. M., and S. E. Belcher (2004), Time-dependent, coupled, Ekman boundary layer solutions incorporating Stokes drift, *Dyn. Atmos. Oceans* , *37*, 313–351, doi:10.1016/j.dynatmoce.2003.11.001.

Liu, Y., R. H. Weisberg, S. Vignudelli, and G. T. Mitchum (2014), Evaluation of altimetry-derived surface current products using Lagrangian drifter trajectories in the eastern Gulf of Mexico, *J. Geophys. Res. Oceans*, *119*, 2827–2842, doi:10.1002/2013JC009710.

Lumpkin, R., A. S. Grodsky, L. Centurioni, M. H. Rio, J. A. Carton, and D. Lee (2012), Removing spurious low-frequency variability in drifter velocities JTECH-D-12-00139.

Maximenko, N., P. Niiler, M.-H. Rio, O. Melnichenko, L. Centurioni, D. Chambers, V. Zlotnicki, and B. Galperin (2009), Mean dynamic topography of the ocean derived from satellite and drifting buoy data using three different techniques, *J. Atmos. Oceanic Technol.*, *26*, 1910–1919, doi:10.1175/2009JTECHO672.1.

Mulet, S., M.-H. Rio, and S. Bruinsma (2012), Accuracy of the preliminary GOCE GEOID models from an oceanographic perspective, *Mar. Geod.*, *35*, 314–336, doi:10.1080/01490419.2012.718230.

Niiler, P. P., R. Davis, and H. White (1987), Water following characteristics of a mixed layer drifter, *Deep Sea Res., Part I*, *34*, 1867–1881, doi:10.1016/0198-0149(87)90060-4.

Niiler, P. P., A. S. Sybrandy, K. Bi, P.-M. Poulain, and D. Bitterman (1995), Measurements of the water-following capability of holey-sock and TRISTAR drifters, *Deep Sea Res., Part I*, *42*, 1951–1964.

Park, J. J., K. Kim, and B. A. King (2005), Global statistics of inertial motions, *Geophys. Res. Lett.*, *32*, L14612, doi:10.1029/2005GL023258.

Ralph, E. A., and P. P. Niiler (1999), Wind-driven currents in the tropical Pacific, *J. Phys. Oceanogr.*, *29*, 2121–2129, doi:10.1175/1520-0485.

Rio, M. H., S. Guinehut, and G. Larnicol (2011), New CNES-CLS09 global mean dynamic topography computed from the combination of GRACE data, altimetry, and in situ measurements, *J. Geophys. Res.*, *116*, C07018, doi:10.1029/2010JC006505.

Rio, M.-H. (2012), Use of altimeter and wind data to detect the anomalous loss of SVP-type drifter's drogue, *J. Atmos. Oceanic Technol.*, *29*, 1663–1674, doi:10.1175/JTECH-D-12-00008.1.

Rio, M.-H., and F. Hernandez (2003), High-frequency response of wind-driven currents measured by drifting buoys and altimetry over the world ocean, *J. Geophys. Res.*, *108*(C8), 3283–3301, doi:10.1029/2002JC001655.

Rossby, C. G., and R. B. Montgomery (1935), *The Layer of Frictional Influence in Wind and Ocean Currents*, *Papers Phys. Oceanog. Meteorol.*, vol. 3, 101 pp., Massachusetts Institute of Technology and Woods Hole Oceanographic Institution, Cambridge, Mass.

Schaeffer, P., Y. Faugère, J. F. Legeais, A. Ollivier, T. Guinle, and N. Picot (2012), The CNES_CLS11 global mean sea surface computed from 16 years of satellite altimeter data, *Mar. Geod.*, *35*, 3–19, doi:10.1080/01490419.2012.718231.

Simmons, A., S. Uppala, D. Dee, and S. Kobayashi (2007), ERA-Interim: New ECMWF reanalysis products from 1989 onwards, *ECMWF Newsl.*, *110*, 25–35.

Sudre, J., and R. Morrow (2008), Global surface currents: A high resolution product for investigating ocean dynamics, *Ocean Dyn.* , *58*, 101–118, doi:10.1007/s10236-008-0134-9.

Sudre, J., C. Maes, and V. Garcon (2013), On the global estimates of geostrophic and Ekman surface currents, *Limnol. Oceanogr. Methods*, *3*, 1–20, doi:10.1215/21573689-2071927.